Computer Methods and Programs in Biomedicine 231 (2023) 107409

Contents lists available at ScienceDirect

Computer Methods and Programs in Biomedicine

journal homepage: www.elsevier.com/locate/cmpb

Unveiling the effects of key factors in enhancing gastroesophageal reflux: A fluid-structure analysis before and after laparoscopic sleeve gastrectomy

Ilaria Toniolo[a,b,1], Alice Berardo[b,c,d,*], Michel Gagner[e], Mirto Foletto[b,f,g], Emanuele Luigi Carniel[a,b]

[a] Department of Industrial Engineering, University of Padova, Italy
[b] Centre for Mechanics of Biological Materials, University of Padova, Italy
[c] Department of Civil, Environmental and Architectural Engineering, University of Padova, Italy
[d] Department of Biomedical Sciences, University of Padova, Italy
[e] Department of Surgery, Hôpital du Sacré-Coeur de Montréal, Canada
[f] Department of Surgery, Oncology and Gastroenterology, University of Padova, Italy
[g] IFSO Bariatric Centre of Excellence, Policlinico Universitario, University of Padova, Italy

ARTICLE INFO

Article history:
Received 19 September 2022
Revised 3 February 2023
Accepted 6 February 2023

Keywords:
Computational modelling
Fluid-structure interaction
Bariatric surgery
Gerd
His-angle
Bolus viscosity

ABSTRACT

Background and Objectives: Gastro-oesophageal reflux disease (GERD) consists in the passage of gastric acid content from the stomach to the oesophagus, causing burns and deteriorating the quality of life. Laparoscopic Sleeve Gastrectomy (LSG) could induce *de novo* GERD and worsen pre-existing GERD because of the higher gastric pressurisation, reduction of stomach volume and a wider His-angle. In the proposed work, various computational gastric 2D models were developed to understand the effects of variables such as the His-angle, the antral dimension, and the bolus viscosity on the reflux increase.
Methods: Fluid-Structure Interaction (FSI) computational models which couple the solid mechanics of the gastric wall, and the fluid domain of the bolus, have been developed to shed light on biomechanical aspects of GERD after LSG. A closure was imposed to the lower oesophageal sphincter (LES) mimicking what happens physiologically after food intake.
Results: Results showed that the configuration prone to higher reflux flow was the post-surgical 65° model with a staple line starting directly from the pylorus without antral preservation, for all considered viscosities. Increasing viscosity, reflux flow decreased. Post-surgical refluxes were higher than pre-ones and decreased with increasing antrum preservation.
Conclusions: These results could be a starting point for analysis of anatomical features, bariatric surgery and GERD occurrence. Further studies based on 3D geometries need to be performed.

1. Introduction

Gastro-oesophageal Reflux Disease (GERD) has a global impact on health costs and worsen health-related quality of life. Ranges of GERD prevalence estimates were 18.1–27.8% in North America, 8.8–25.9% in Europe, 2.5–7.8% in East Asia, 8.7–33.1% in the Middle East, 11.6% in Australia and 23.0% in South America [1]. Disease manifestations vary depending on the severity and magnitude of reflux [2]. The Montreal Definition of GERD states that it is a condition developed when the reflux of stomach contents causes troublesome symptoms and/or complications [3]. The spectrum of GERD has expanded into a group of syndromes differentiated by manifestations of reflux disease [2]. In the literature, magnetic resonance imaging and high-resolution manometry can assess esophagogastric motility and the extent of GERD. A wider His-angle, a larger Esophago-Gastric Junction (EGJ) opening, a slower gastric emptying rate and a smaller Lower oesophageal Sphincter (LES) pressure promote GERD [4]. The increase in prevalence of severe obesity and the subsequent larger Bariatric Surgery (BS) demand may worsen the appearance of reflux disease, since pre-operative GERD diagnosis is a risk factor for post-operative oesophageal dis-

Abbreviations: GERD, Gastro-oesophageal Reflux Disease; LSG, Laparoscopic sleeve gastrectomy; EGJ, Esophago-gastric junction; BS, Bariatric surgery; CFD, computational fluid dynamics; LES, Lower oesophageal phincter; FSI, Fluid-structure interaction.

* Corresponding author.
E-mail address: alice.berardo@unipd.it (A. Berardo).
[1] *Current affiliation:* Department of Civil, Environmental and Architectural Engineering, University of Padova, Italy.

https://doi.org/10.1016/j.cmpb.2023.107409
0169-2607/

ease after BS and bariatric procedures and endoluminal bariatric therapies have been associated with increased GERD symptoms [5,6].

In 2015–2016, the prevalence of obesity in US was 39.8% in adults and 18.5% in youth [7] and it is one of the risk factors for GERD, which has resulted in a significant increase in the incidence of GERD worldwide [8]. Laparoscopic Sleeve Gastrectomy (LSG) is a well-established primary bariatric procedure [9] that is considered easy to perform and allows for early discharge [10]. However, LSG has shown the highest rate of *de novo* GERD [6], due to both an increase in the EGJ angle, a significant reduction of the stomach. In fact, about 6 months after LSG, the angle between EGJ and gastric fundus (His-Angle) tends to increase from approximately 35° to 51°, while the gastric capacity is reduced by more than 80%, resulting in intragastric pressure enhancement. These changes seem to be correlate to reflux events [11]. A factor which can counterbalance this event is a faster gastric emptying, which depends on post-LSG antral dimension. The final antrum size is linked to the distance from the pylorus to the division line between the sleeved stomach, which becomes the new stomach, and the resected stomach, or the portion which is removed from the bariatric patient. This distance varies from 2 to 6 cm [12] depending on the surgeon's evaluation. A higher antral preservation (6 cm from pylorus) showed a faster gastric emptying rate, but less incidence of GERD symptoms (with no significant difference) with respect to patients whom antral resection of 2 cm from pylorus was adopted [13]. In general, rapid gastric emptying with asymptomatic deglutitive is common following LSG [14]. Starting from these considerations, different tricks in LSG procedure have been introduced to decrease GERD-related side effects, such as the use of a staple-line reinforcement product, oversewing of the staple line, different bougie sizes and different distances from the pylorus where stapling is initiated [15]. On the other hand, the Montpellier bariatric team has recently proposed the Nissen-Sleeve (N-Sleeve) to offer patients an alternative in case of contraindication to Roux-en-Y gastric bypass (RYGBP) [16,17] and, in general, new LSG techniques proposing fundoplication are spreading [18,19]. However, these two latter techniques are not well-established yet and they are performed only in bariatric patients with severe GERD. More studies are necessary to assess their effectiveness and reliability.

In the literature, solid mechanical computational models of the gastric district were fully described [20–23], but computational fluid dynamics (CFD) and fluid-structure interaction (FSI) computational models of stomach that correlate EGJ, BS and GERD still lack. Most of CFD studies stressed on the flow dynamics during the process of mixing liquid foods with the gastric juice [24,25] or to investigate the change of the flow dynamics in respect to viscosity [26] taking into account the active contractile behaviour of the gastric wall. An initial CFD work on the EGJ was published but it did not consider a dynamic change in the EGJ, relegating it to only a preliminary study [27]. For these reasons, the aim of this paper is to fill the gap evaluating computationally the fluid dynamics of the bolus respect to the His-angle and the viscosity, in pre- and post-surgical conditions, accounting for FSI phenomena. The post-surgical analysis considered a 40-Fr LSG procedure and its state-of-art possible post-surgical configurations depending on the distance between the pylorus and staple line. Computational models could highlight the main issues related to BS improving the success rate without performing preliminary time-consuming and expensive experimental campaigns on animal and human beings [28].

2. Materials and methods

2.1. Geometrical models

From a pre-surgical average stomach geometry reported in literature [21,29], a 2D model was extracted by means of Solidworks® (Dassault Systemes, 2018), and a 20 mm-withd and 138 mm-long oesophageal tract was added, which included the LES region (about 30 mm length [30–33]), which is a high-pressure zone located in the distal part of oesophagus in the distal part. The mean thickness of the gastric and oesophageal wall was 1.3 mm, providing for the solid region of the model. Multiple geometries were realized by differing the inclination of the oesophageal tract, which led to different His-angles, measured as the angle formed by the closest part of the fundus to oesophagus and the oesophageal tract as drawn in the Fig. 1b. Angles ranged between 25° and 65°, with two intermediate situations (30° and 45°), to analyse similar values reported by Quero et al. [11] (Fig. 1a to 1d). The sleeved stomachs were drawn as extension of the oesophageal tract (Fig. 1e), simulating the use of a 40-Fr (13.3 mm) bougie size [21,34], then variating the antrum region. The configurations were identified as "post", "post 2cm" and "post 6cm" when the LSG staple line started directly from the pylorus or it was 2 and 6 cm distant from the pyloric value, respectively.

The bolus was assumed as a viscous liquid which occupies all the intraluminal volume of both stomach and oesophagus. One internal point was added to all the geometries in the corpus, for the application of the intraluminal pressure conditions.

2.2. FSI governing equations

Fluid-Structure Interaction multiphysics coupling combines fluid flow with structural mechanics to capture the interaction between the fluid and the solid structure, thus it appears as an additional condition on the boundaries between the fluid and the solid.

The equations of motion for a single-phase fluid are the continuity equation and the momentum equation, respectively (in divergency form):

$$\frac{\partial \rho}{\partial t} + \nabla \cdot \left(\rho\ u_{fluid}\right) = 0 \tag{1}$$

$$\rho \frac{\partial u_{fluid}}{\partial t} + \rho u_{fluid} \cdot \nabla u_{fluid} = -\nabla p + \nabla \cdot \left(\mu(\nabla u_{fluid} + (\nabla\ u_{fluid})^T) - \frac{2}{3}\mu\left(\nabla \cdot u_{fluid}\right)I\right) + F \tag{2}$$

where ρ is the density (kg/m^3), u_{fluid} is the velocity vector (m/s), p is pressure (Pa), F is the volume force vector (N/m^3). These equations are applicable for incompressible as well as for compressible flow with density and viscosity variations. The hypothesis of an incompressible fluid and a constant density ρ simplifies the previous equilibrium equations in:

$$\rho \nabla \cdot u_{fluid} = 0 \tag{3}$$

$$\rho \frac{\partial u_{fluid}}{\partial t} + \rho\left(u_{fluid} \cdot \nabla\right)u_{fluid} = \nabla \cdot \left[-pI + \mu\left(\nabla u_{fluid} + \left(\nabla u_{fluid}\right)^T\right)\right] + F \tag{4}$$

These equations describe the fluid-dynamic physics. To couple the solid mechanics physics in order to have a multiphysics model (FSI), the following equation has to be added:

$$-\nabla \cdot \sigma = F_V \tag{5}$$

σ is the stress tensor, defined as $J^{-1}FSF^T$, where F is the deformation gradient, J is the Jacobian defined as the *det(F)*, and S is the second Piola–Kirchhoff. S is defined as the partial derivative of the strain energy potential (W) respect to the Green-Lagrange strain tensor : $S = \frac{\partial W}{\partial E}$. Finally, F_v is the force per unit volume (N/m^3).

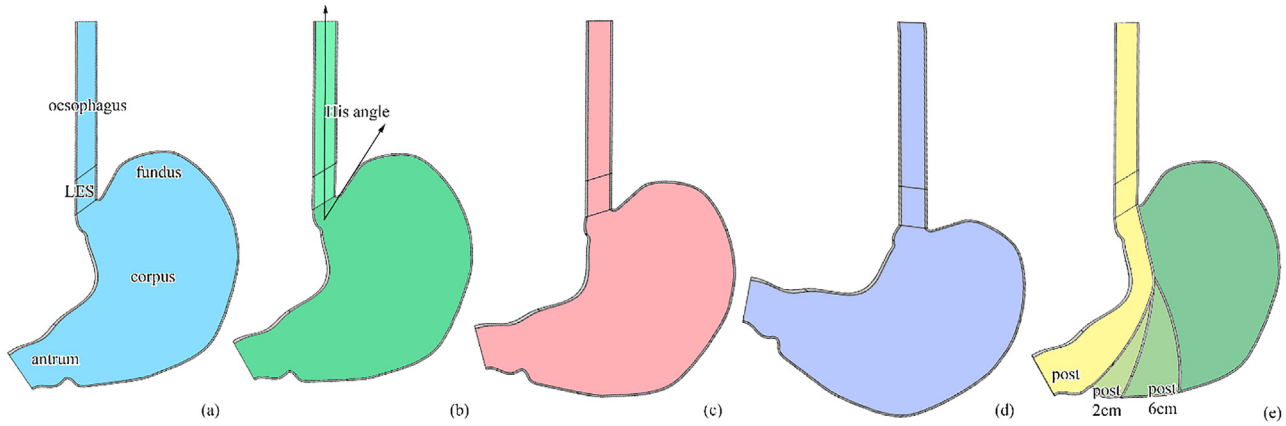

Fig. 1. 2D models of pre- and post-surgical configurations (post, post 2 cm and post 6 cm), considering different His-angles: 25° (a), 30° (b and e), 45° (c) and 65° (d).

Table 1
Material properties: Ogden coefficients for the different stomach regions and oesophagus.

Region	α [-]	μ [kPa]
Oesophagus	6.74	75.58
Fundus	8.11	7.98
Corpus	8.64	9.52
Antrum	6.95	5.94

2.3. Solid mechanics constitutive formulation

From the results obtained during experimental activities on human tissues of patients with morbid obesity during uniaxial tests [23,35], average mechanical behaviours were derived by combing the circumferential and longitudinal behaviour of the different regions composing the stomach (fundus, corpus and antrum) in order to simplify the gastric tissues as an isotropic hyperelastic material. These stress-strain curves were fitted with a first order Ogden material model ($N = 1$) and the parameters obtained are reported in Table 1. The form of the Ogden strain energy potential W is reported in the following equation:

$$W = \frac{2\mu}{\alpha^2}\left(\bar{\lambda}_1^{\alpha} + \bar{\lambda}_2^{\alpha} + \bar{\lambda}_3^{\alpha} - 3\right) + \frac{1}{D}(J^{el} - 1)^2$$

where $\bar{\lambda}_i$ are the deviatoric principal stretches $\bar{\lambda}_i = J^{-1/3}\lambda_i$; λ_i are the principal stretches; and μ, α and D are material parameters.

2.4. Fluid behaviour

Comsol Multiphysics 5.4 (Comsol Inc., Burlington, MA, USA) was the software utilized to run the FSI simulations. An incompressible homogeneous single-phase laminar flow characterized by a density of 1000 kg/m^3 was assigned. Different dynamic viscosity values were tested to simulate the intake of different kind of food [36]. The chosen values were 0.1, 1 and 10 Pa·s, which indicate different types of fluid food: orange juice, yogurt, and rice pudding, respectively. A No-Slip condition ($u_{fluid} \cdot n = 0$ and $[-pI + \mu(\nabla u_{fluid} + (\nabla u_{fluid})^T)]\, n = 0$) was imposed to have a fluid velocity equal to zero in proximity of the solid domain walls.

2.5. Boundary conditions and constrains

Interpolation functions (namely, *oesophagus, corpus_pre* and *corpus_post,* as reported in Fig. 2) were established to characterize the main esophagogastric regions in terms of pressure, obtained from high-resolution manometry measurements in post-prandial conditions [11,37–39]. The first function imposes the prescribed pressure in the inlet, while the second or the third define the intragastric pressure in pre- either post-surgical configuration. To simulate the action of diaphragm muscles on the distal part of the oesophagus to close the gastroesophageal junction, a prescribed displacement was applied to LES region, which corresponded to a closure of 90% of the internal diameter. The duration of the simulation (which does not correspond to a real physiological time for the gastric response, but only from a computational reliability) was imposed equal to 100 s to reach the equilibrium response. From 0 to 1.5 s, the oesophagus and corpus reached the maximum pressure and then remained constant, while from 0 to 7.5 s the LES reached the maximum closure and then remained constant (Fig. 2). An external boundary spring foundation condition was imposed to enforce the role of surrounding organs, with the only exception for the LES region. The inlet was set in the proximal part of the oesophagus, while the outlet was defined in the connection of the stomach to duodenum, with null velocity as boundary condition (thus considering no stomach emptying). An additional prescribed displacement condition was applied at the solid domains next to inlet and outlet port imposing a null displacement.

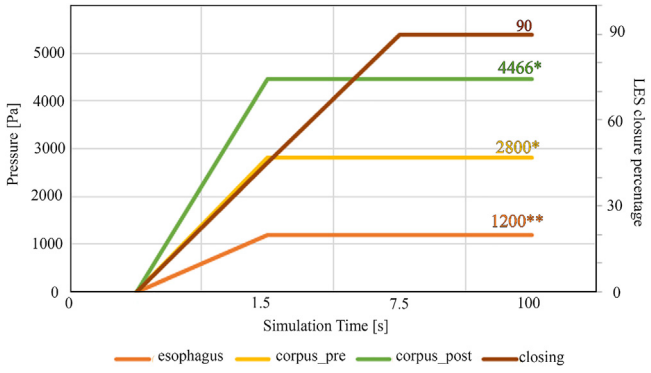

Fig. 2. Interpolation functions established to characterize the main esophagogastric regions in terms of pressure. * indicated that the pressures were extracted from Quero et al. [11], while ** was set by means of high-resolution manometry measurements in post-prandial conditions [37–39].

2.6. Meshing operation

A triangular extra-fine mesh was chosen which accounted for a minimum element size of 0.02 mm up to a maximum of 2.15 mm with a grow factor of 1.08 for the gastric district, while for the oe-

sophageal tract the minimum and the maximum size were 0.25 and 0.4 mm, respectively. The discretization to finite elements was finer to properly characterize the region where the reflux took place. A boundary layer of five elements was imposed to properly define the interface behaviour of the liquid phase. The moving mesh was imposed selecting the whole fluid domain.

Mesh sensitivity analysis was performed with the automatic meshing tool provided by the software, from an extra coarse to extra fine mesh (from a maximum element size of 39 and 23 mm, to 0.2 and 0.2 mm, for the mechanical and fluid domain respectively). The mesh analysis revealed that the results of extra fine and very fine mesh did not vary significantly. Hence, the chosen element size fall into the values reported at the initial of the paragraph, related to a very fine mesh for the gastric region, while to an extra-fine mesh for the gastro-oesophageal region, where the reflux flow was measured.

2.7. Numerical simulations

Simulations were performed with Comsol Multiphysics 5.4 (Comsol Inc., Burlington, MA, USA), time-dependant, direct (PARDISO method), non-linear (automatic Newton method) and fully-coupled solver, with time step automatically computed which varied along the simulation between 0.018 s to 3 and 297,749 degrees of freedom.

2.8. Data processing

Reflux flow was computed as integral calculated on the half of the "horizontal" line, which delimited the most proximal part of oesophagus. To calculate the simplified 3D flux through the oesophagus from the 2D model, the first Pappa-Guldino theorem was applied [40] in order to compute the transversal area of the oesophagus canal from 2D model by considering a 360° rotation of the half distal oesophagus curve.

3. Results

When considering food intake, a pressure drop between the stomach and oesophagus is established leading to a flux from the stomach to the oesophagus canal that can be linked to potential gastric reflux (Fig. 3). From the FSI simulations, the fluid flux (cm^3/s) at the equilibrium was obtained, once the LES closes almost completely (90%) and the velocity stabilizes (Fig. 2, after 100 s). The flow calculated at the proximal part of the oesophagus depends on physiological features, e.g., His-angle, pressure drop along the canal and by viscosity. In addition, if LSG is performed, a considerable variation of the post-surgical stomach shape is induced, with a strong volumetric capacity reduction, which leads to a higher pressurization in correspondence of a less amount of food (Fig. 3c) [11]. In addition, the stomach change into a tubular shape may alter the His-angle, with significant changes in the velocity field (Fig. 3b).

When comparing all the pre-surgical configurations, the final flux increases accordingly to the increase in the His-angle, up to two orders of magnitude (Fig. 4, green bars).

However, lower values of the flux were observed in the post-surgical models, both imposing a gastric pressure in the post-surgical models equal to that characterizing the pre-surgical stomach (2800 Pa) and in case of a higher pressure, typical of sleeved stomachs (4466 Pa) (Fig. 4b and a, respectively).

Fig. 4a shows the variation of the flux when moving from 25° to 65° in pre- and post-surgical models with a different intragastric pressure (2800 Pa and 4466 Pa respectively) and 1 Pa·s fluid viscosity. Results highlighted a flux increase up to 170 times for 25° until about 2 times for 65°, with a pronounced decreasing trend as the His-angle widened.

When the intragastric pressure was the same between pre- and post-surgical models, only in the presence of the 65° it was observed a higher flux (20% more) before the LSG rather than the corresponding post-surgical model (Fig. 4b). On the contrary, in the other configurations, the flux resulted almost 80 times greater in 25°, until about 12% more in 45° (same viscosity as Fig. 4a). Fig. 4c and d reported the flux variations when a fluid with a smaller or grater viscosity (0.1 and 10 Pa·s, respectively) was considered. With a greater viscosity, the flux in post-surgical configurations with reference to the pre-surgical ones, increased up to 206% (25°), 268% (30°), 145% (45°) and 91% (65°), while numbers became evenly greater with a 0.1 Pa·s viscosity.

Furthermore, post-surgical configurations differed in the antrum size, in order to assess its influence in flux amount. Models with the major antrum dimension (post 6 cm configuration) recorded the lowest flux amongst all post-surgical conformations with same His-angle. However, these values did not change significantly, showing a feeble decreasing trend at the increase in antrum region size (Fig. 4, blue, yellow and dark blue bars).

4. Discussion

Among the bariatric operations performed worldwide, LSG is associated with higher risk of postoperative GERD and esophagitis compared with other bariatric operations [5]. LSG provides a strong reduction in the volumetric capacity of the stomach, which impacts on the intragastric pressure and widens the His-angle in the long run. The anatomy and the orientation modification, combined with the increase in intragastric pressure, promote reflux events also in patients with severe obesity, who did not suffer from GERD before LSG. The top five ranked GERD predictors after LSG are age, weight, preoperative GERD, size of orogastric tube, and distance of first stapler fringe from the pylorus [41]. In the proposed work, only the factors which can be introduced in a FSI simulations were considered, namely bougie size, and distance of first stapler fringe from the pylorus, viscosity and His-angle.

From the simulations, a reverse fluid flux from the stomach to the oesophagus canal was observed due to the imposed initial conditions consisting in a pressure drop among the two regions and a partially closed (90%) LES. The aim was to analyse how the reverse flux varied according to pre- and post-surgical configurations, His-angle, antral dimension and bolus viscosity.

Accordingly to clinical evidence [4], a wider His-angle in the pre-surgical configuration resulted in a greater flux flow, stating that the physiological shape of the stomach could represent one of the first causes for possible reflux (e.g., GERD).

Including the effects of shape modification after LSG, even higher flux values were observed, both if considering or not the higher pressurisation of post-surgical configurations due to volume reduction and the completely removal of fundus (the most compliant region) (Fig. 4b and a, respectively). In the first analysis, the only affecting variable was the stomach geometry and the post-surgical models recorded higher values of reflux flow, with the only exception for 65° Indeed, the variation between pre- and post-surgical configurations of the flux flow decreased when moving from 25° (7300%) to 45° (12%) and became even negative for 65°(−11%). This outcome suggested that the potential reflux is strongly influenced by a high variation of the His-angle, combined with the volume reduction; however, when wider angles were present (i.e., 65°), this effect became slighter, indicating that reflux increase could be generated by other factors.

However, LSG induces also an increase in intragastric pressure (*in-vivo* manometry reported approximately double values [11] after LSG), thus the combination of greater pressure with the His-

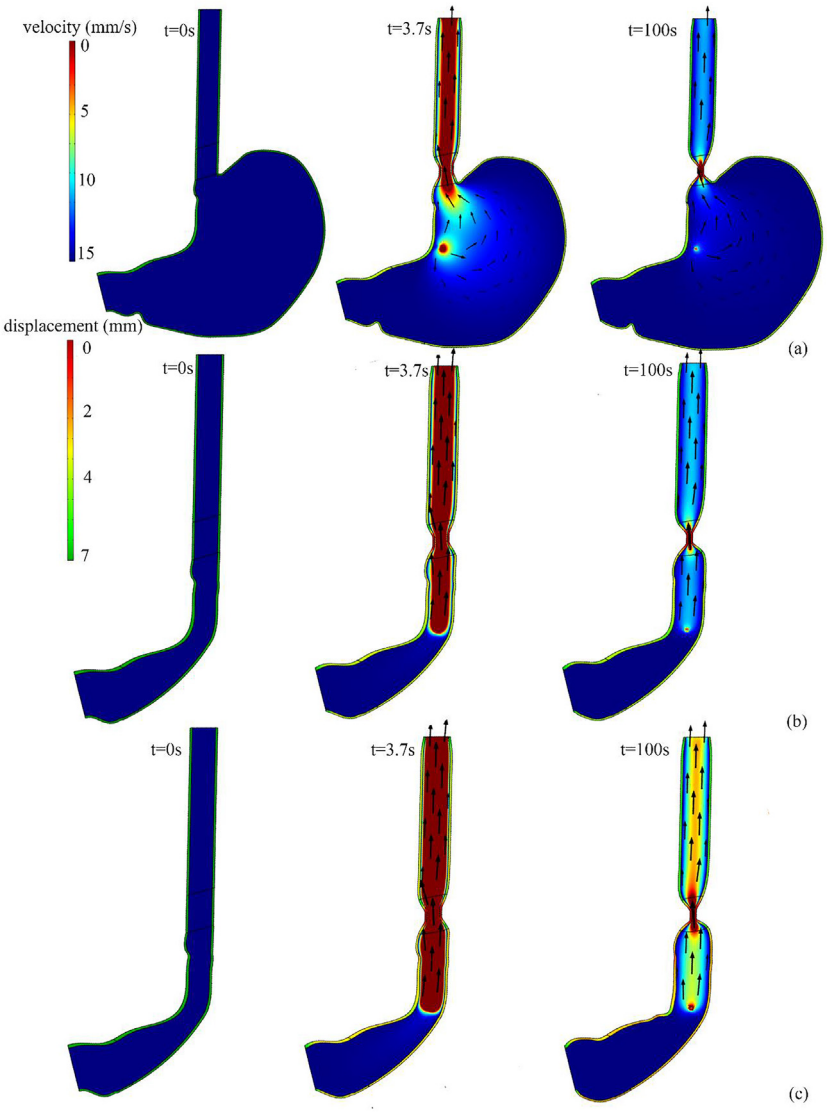

Fig. 3. Colormaps of the velocity (for the fluid domain) and the displacement (for the solid domain) in the 45° His-model in pre- and post-surgical configurations at different moments of the simulation: initial ($t = 0$ s), in the middle of the LES closing ($t = 3.75$ s) and at the equilibrium final point ($t = 100$ s) in case of viscosity equal to 1 Pa·s. The intragastric pressure was 2800 Pa in (a) and (b), while it was 4466 Pa in (c).

angle variations proved the maximum flux flow with respect to the previous scenario (Fig. 4). Even if to date no clinical measurements were obtained to quantify the reflux, these results propose that this potential inverse flux could be directly linked to reflux events, being in agreement with the *"de novo"* GERD after LSG.

If a larger antrum region was preserved after the surgery, a lower final flux was observed for all the His-angle configurations respect to other post-surgical configurations, which could discourage reflux after food intake. This effect is induced by a closer similarity of the final gastric shape to the pre-surgical one, where lower flux flows were recorded. Therefore, geometrical features (e.g., His-angle, fundus removal and antral final dimension) appeared to affect the fluid-dynamics of the stomach, promoting the rising of the liquid contents, even if no higher pressures are included.

Another key factor in enhancing potential reflux from the stomach is fluid viscosity. As expected by Eq. (4), the flux magnitude varied inversely proportional to fluid viscosity, with significant changes when moving from lower (0.1 Pa·s) to higher (10 Pa·s) values. Accordingly to the here reported results, Shimizu et al. [42] observed that semisolid formulae with viscosity around 6 Pa·s significantly reduced the incidence of gastroesophageal reflux, thus reducing the risks of GERD. Moreover, a marked delay in oesophageal transport with increasing viscosity of the bolus was also reported in [43], where, with conventional oesophageal manometry and impedance monitoring, the effect of bolus viscosity on oesophageal motility and bolus transit was assessed, confirming that the velocity of oesophageal bolus transport and motility decreased with increasing bolus viscosity. Viscosities adopted within this study referred to common fluid food, with reference to these previous studies.

However, after a meal, the viscosity is not the only food variable promoting or reducing reflux, but also pH and the presence of solid particles should be considered for a better and complete understanding of the bolus effects in potential reflux events. Other assumptions were realized in the present work, since we limited to 2D stomach model instead of the 3D, thus not including the influence of a realistic and complete geometry of the organ. Additional aspects should be further discussed, as the influence of the adopted boundary conditions, and the lack of gastric active motility

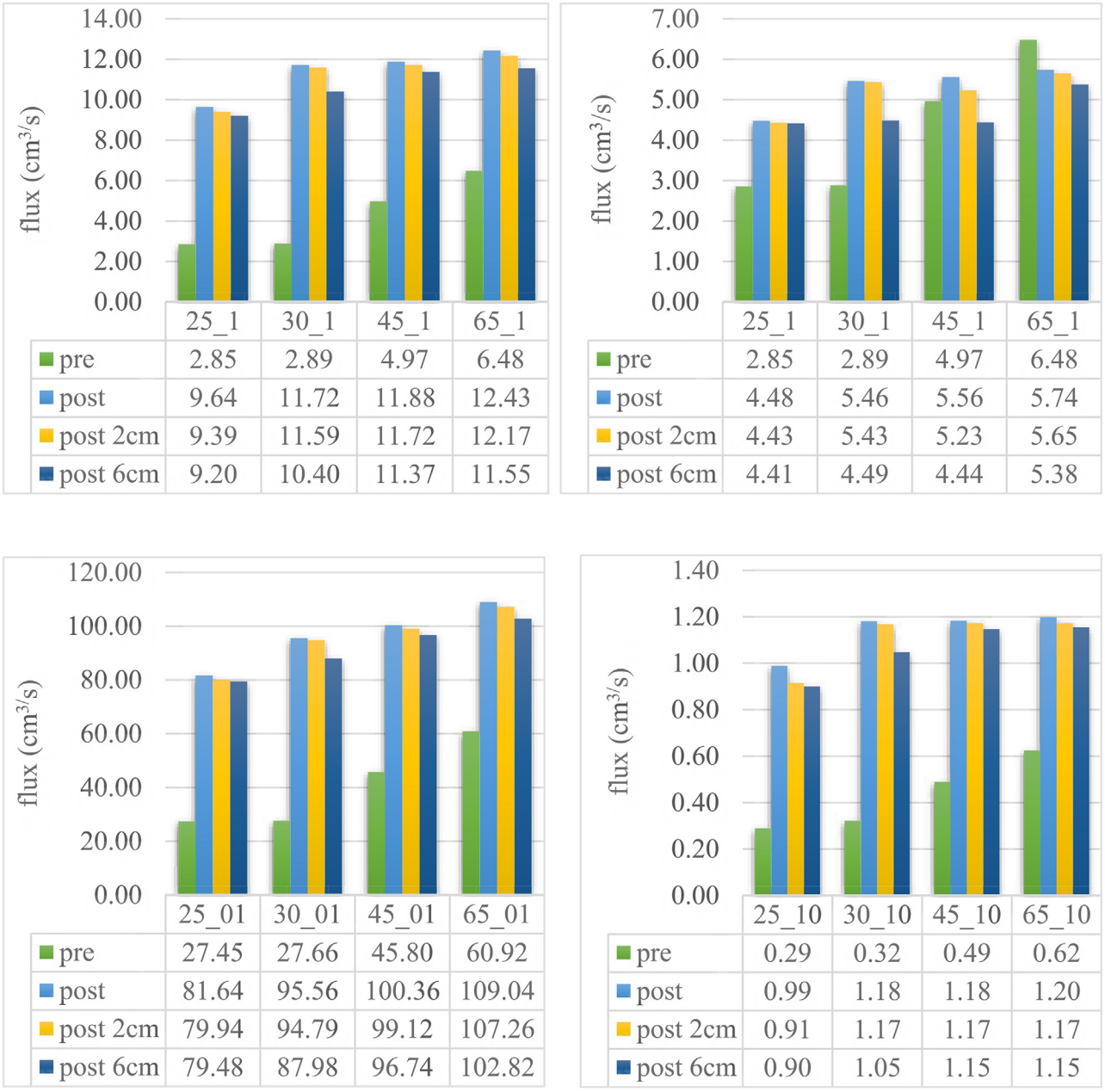

Fig. 4. Reflux flows of the pre- and post-surgical models when the intragastric pressure was 2800 Pa for physiological models and 4466 Pa for sleeved stomachs. Bolus viscosity was equal to 1 Pa·s (a), Reflux flows of the pre- and post-surgical models when the intragastric pressure was 2800 Pa in all models and bolus viscosity was equal to 1 Pa·s (b), Reflux flows of the pre- and post-surgical models when the intragastric pressure was 2800 Pa for physiological models and 4466 Pa for sleeved stomachs. Bolus viscosity was equal to 0.1 Pa·s (c), Reflux flows of the pre- and post-surgical models when the intragastric pressure was 2800 Pa for physiological models and 4466 Pa for sleeved stomachs. Bolus viscosity was equal to 10 Pa·s (d).

and gastric emptying, which could lead to possible overestimations of the expected flux due to the absence of both mixing effects and flux through pylorus.

This is a simplification of a realistic situation, since liquids usually pass through the pyloric sphincter after few minutes from the ingestion [44], but justified since the aim was to analyse the worst configuration with the maximum reflux (since no other fluxes are occurring in the same time). Gastric emptying will be added in the future studies because its role in GERD development. Notwithstanding, the interest was primary focused to unveil the potential factors in enhancing the flux rather than to quantify this latter. Indeed, since no measurements of the reflux flow are available from a clinical point of view, it is possible to infer that, despite this simplification, the proposed models are able to draw the attention on the effects of single and combined features on the potential gastroesophageal reflux, especially after quite invasive bariatric surgeries.

5. Conclusions

Within this work we provided a computational evaluation of several effects that could induce or reduce a potential reflux from the stomach to the oesophageal canal during a post meal simulation, especially for people affected by morbid obesity candidates for LSG. As reported in some works [6,8,11], after LSG patients could develop "*de novo*" GERD due to non-negligible morphological changes of the His-angle and stomach volume. Moreover, the sleeved stomach after LSG usually shows higher intragastric pres-

sures after food intaking with respect to pre-surgical ones, even though the amount of food is significant lower. These aspects appeared relevant to generate a greater flux, both as single, but also as coupled effects. Moreover, other factors may be crucial for reflux events too, such as the bolus viscosity. Being the first yet preliminary fluid-structure interaction study of the digestive tract, this research aimed at analysing how geometry and fluid properties combined with LSG affected the reflux events in a coupled solid and fluid-dynamic point of view, suggesting that His-angle greatly affects the reflux flow in the presence of the same fluid viscosity. In addition, also fluid viscosity plays an important role in the reverse flux, changing it of some orders of magnitude lower (with an increase in the viscosity) or higher (with a decrease in viscosity). For a complete characterization, future studies should consider a 3D geometry, based on *in vivo* organ segmentation [45], the pressure contribution of antrum region and pylorus, and possible correlations to pH and gastric motility. However, this first computational assessment was able to clarify the role of these key points in stomach fluid dynamics, showing the importance to forecast possible GERD development, especially after LSG, for a better clinical practice.

Authors disclosure

All authors have given approval to the final version of the manuscript. The authors Ilaria Toniolo, Alice Berardo, Mirto Foletto and Emanuele Luigi Carniel have no conflicts of interest or financial ties to disclose. Michel Gagner is a consultant for GT Metabolic Solutions Inc and Lexington Medical.

Declaration of Competing Interest

Michel Gagner is a consultant for GT Metabolic Solutions Inc and Lexington Medical. The other authors declare no conflict of interest.

Acknowledgments

This work was supported by MIUR, FISR 2019, Project n FISR2019_03221, titled CECOMES: CEntro di studi sperimentali e COmputazionali per la ModElliStica applicata alla chirurgia and by the Department of Civil, Environmental and Architectural Engineering, University of Padova, BIRD2022 “Computational gastric biomechanics to improve bariatric surgery procedures with a patient-specific approach”.

References

[1] H.B. El-Serag, S. Sweet, C.C. Winchester, J. Dent, Update on the epidemiology of gastro-oesophageal reflux disease: a systematic review, Gut 63 (2014) 871–880, doi:10.1136/gutjnl-2012-304269.

[2] N. Vakil, Disease definition, clinical manifestations, epidemiology and natural history of GERD, Best Pract. Res. Clin. Gastroenterol. 24 (2010) 759–764, doi:10.1016/j.bpg.2010.09.009.

[3] S.V. Van Zanten, P. Kahrilas, J. Dent, R. Jones, N. Vakil, L. Agreus, D. Armstrong, S. Attwood, J.F. Bergman, M.A. Bigard, P. Blount, P. Bytzer, T. Chiba, G. Delle Fave, H. El-Serag, D. Fan, R. Fass, N. Flook, J.P. Galmiche, M. Hongo, F.H. Iga, J. Jankowski, D. Johnson, F. Johnssorn, P. Katelaris, Y. Kinoshita, E. Klinkenberg-Knol, J. Labenz, H. Liker, P. Malfertheiner, H. Miwa, P. Moayyedi, F. Pace, J. Prado, J. Richter, G. Salis, L. San-Ren, P. Sharma, V. Stanghellini, J. Tack, N. Talley, B. Wong, Y. Yaozong, C. Zapata, Die Montreal-definition und -klassifikation der gastroösophagealen refluxkrankheit: ein globales evidenzbasiertes konsensus-papier, Z. Gastroenterol. 45 (2007) 1125–1140, doi:10.1055/s-2007-963633.

[4] J. Curcic, S. Roy, A. Schwizer, E. Kaufman, Z. Forras-Kaufman, D. Menne, G.S. Hebbard, R. Treier, P. Boesiger, A. Steingoetter, M. Fried, W. Schwizer, A. Pal, M. Fox, Abnormal structure and function of the esophagogastric junction and proximal stomach in gastroesophageal reflux disease, Am. J. Gastroenterol. 109 (2014) 658–667, doi:10.1038/ajg.2014.25.

[5] L.A. Bevilacqua, N.R. Obeid, J. Yang, C. Zhu, M.S. Altieri, K. Spaniolas, A.D. Pryor, Incidence of GERD, esophagitis, Barrett's esophagus, and esophageal adenocarcinoma after bariatric surgery, Surg. Obes. Relat. Dis. 16 (2020) 1828–1836, doi:10.1016/j.soard.2020.06.016.

[6] M.I. Itani, J. Farha, M.K. Marrache, L. Fayad, D. Badurdeen, V. Kumbhari, The effects of bariatric surgery and endoscopic bariatric therapies on GERD: an update, Curr. Treat. Options Gastroenterol. 18 (2020) 97–108, doi:10.1007/s11938-020-00278-y.

[7] C.M. Hales, M.D. Carroll, C.D. Fryar, C.L. Ogden, in: Prevalence of Obesity Among Adults and Youth: United States, National Center for Health Statistics., Hyattsville, MD, 2017, pp. 1–8. 2015–2016. NCHS data brief, no 288NCHS Data Brief.

[8] G. Pavone, N. Tartaglia, A. Porfido, P. Panzera, M. Pacilli, A. Ambrosi, The new onset of GERD after sleeve gastrectomy: a systematic review, Ann. Med. Surg. 77 (2022) 103584, doi:10.1016/j.amsu.2022.103584.

[9] R. Welbourn, D.J. Pournaras, J. Dixon, K. Higa, R. Kinsman, J. Ottosson, A. Ramos, B. van Wagensveld, P. Walton, R. Weiner, N. Zundel, Bariatric surgery worldwide: baseline demographic description and one-year outcomes from the second IFSO global registry report 2013–2015, Obes. Surg. 28 (2018) 313–322 313–322–.

[10] N. Sakran, A. Raziel, O. Goitein, A. Szold, D. Goitein, Laparoscopic sleeve gastrectomy for morbid obesity in 3003 patients: results at a high-volume bariatric center, Obes. Surg. 26 (2016) 2045–2050 2045–2050–, doi:10.1007/s11695-016-2063-x.

[11] G. Quero, C. Fiorillo, B. Dallemagne, P. Mascagni, J. Curcic, M. Fox, S. Perretta, The causes of gastroesophageal reflux after laparoscopic sleeve gastrectomy: quantitative assessment of the structure and function of the esophagogastric junction by magnetic resonance imaging and high-resolution manometry, Obes. Surg. 30 (2020) 2108–2117, doi:10.1007/s11695-020-04438-y.

[12] A. Elgeidie, M. Elhemaly, E. Hamdy, M. El Sorogy, M. Abdelgawad, N. Gadelhak, The effect of residual gastric antrum size on the outcome of laparoscopic sleeve gastrectomy: a prospective randomized trial, Surg. Obes. Relat. Dis. 11 (2015) 997–1003, doi:10.1016/j.soard.2014.12.025.

[13] M.S. Eskandaros, Antrum preservation versus antrum resection in laparoscopic sleeve gastrectomy with effects on gastric emptying, body mass index, and type II diabetes remission in diabetic patients with body mass index 30–40 kg/m^2: a randomized controlled study, Obes. Surg. 32 (2022) 1412–1420, doi:10.1007/s11695-022-05982-5.

[14] Y. Johari, H. Yue, C. Laurie, G. Hebbard, P. Beech, K.S. Yap, W. Brown, P. Burton, Expected values of esophageal transit and gastric emptying scintigraphy post-uncomplicated sleeve gastrectomy, Obes. Surg. 31 (2021) 3727–3737, doi:10.1007/s11695-021-05487-7.

[15] E.R. Berger, R.H. Clements, J.M. Morton, K.M. Huffman, B.M. Wolfe, N.T. Nguyen, C.Y. Ko, M.M. Hutter, The impact of different surgical techniques on outcomes in laparoscopic sleeve gastrectomies: the first report from the metabolic and bariatric surgery accreditation and quality improvement program (MBSAQIP), Ann. Surg. 264 (2016) 464–471, doi:10.1097/SLA.0000000000001851.

[16] I. Ben Amor, V. Casanova, G. Vanbiervliet, J.M. Bereder, R. Habitan, R. Kassir, J. Gugenheim, The nissen-sleeve (N-sleeve): results of a cohort study, Obes. Surg. 30 (2020) 3267–3272, doi:10.1007/s11695-020-04469-5.

[17] N. Musa, D.F. Altomare, Sleeve gastrectomy combined with nissen fundoplication as a single surgical procedure, is it really safe ? a case report, Am. J. Case Rep. (2020) 1–5, doi:10.12659/AJCR.923543.

[18] S. Olmi M.D., M. Uccelli M.D., G.C. Cesana M.D., F. Ciccarese M.D., A. Oldani M.D., R. Giorgi M.D., S.M. De Carli M.D., R. Villa M.D., Modified laparoscopic sleeve gastrectomy with Rossetti antireflux fundoplication : results after 220 procedures with 24-month follow-up, Surg. Obes. Relat. Dis. (2020) 1–10, doi:10.1016/j.soard.2020.03.029.

[19] B. Peng M.D., G. Zhang M.D., G. Chen M.D., Z. Cheng M.D., J. Hu M.D., X. Du M.D., Gastroesophageal reflux disease complicating laparoscopic sleeve gastrectomy : current knowledge and surgical therapies, Surg. Obes. Relat. Dis. 16 (2020) 1145–1155, doi:10.1016/j.soard.2020.04.025.

[20] E.L. Carniel, I. Toniolo, C.G. Fontanella, Computational biomechanics : in-silico tools for the investigation of surgical procedures and devices, Bioengineering 7 (2) (2020) 48 https://doi.org/10.3390/bioengineering7020048.

[21] C. Salmaso, I. Toniolo, C.G. Fontanella, P. Da Roit, A. Albanese, L. Polese, C. Stefanini, M. Foletto, E.L. Carniel, Computational tools for the reliability assessment and the engineering design of procedures and devices in bariatric surgery, Ann. Biomed. Eng. (2020) 48, doi:10.1007/s10439-020-02542-9.

[22] I. Toniolo, C.G. Fontanella, M. Foletto, E.L. Carniel, Biomechanical investigation of the stomach following different bariatric surgery approaches, Bioengineering 7 (2020), doi:10.3390/bioengineering7040159.

[23] I. Toniolo, A. Berardo, M. Foletto, C. Fiorillo, G. Quero, S. Perretta, E.L. Carniel, Patient-specific stomach biomechanics before and after laparoscopic sleeve gastrectomy, Surg. Endosc. (2022), doi:10.1007/s00464-022-09233-7.

[24] C. Li, Y. Jin, A CFD model for investigating the dynamics of liquid gastric contents in human-stomach induced by gastric motility, J. Food Eng. 296 (2021) 110461, doi:10.1016/j.jfoodeng.2020.110461.

[25] C. Li, J. Xiao, X.D. Chen, Y. Jin, Mixing and emptying of gastric contents in human-stomach: a numerical study, J. Biomech. 118 (2021) 110293, doi:10.1016/j.jbiomech.2021.110293.

[26] M.J. Ferrua, R.P. Singh, Modeling the fluid dynamics in a human stomach to gain insight of food digestion, J. Food Sci. 75 (2010) 151–162 151–162–.

[27] B.P. Mcmahon, K.D. Odie, K.W. Moloney, H. Gregersen, Computation of flow through the oesophagogastric junction, World Journal of Gastroenterology 13 (2007) 1360–1364.

[28] E.L. Carniel, I. Toniolo, C.G. Fontanella, Computational biomechanics: in-silico tools for the investigation of surgical procedures and devices, Bioengineering 7 (2020), doi:10.3390/bioengineering7020048.

[29] C.G. Fontanella, C. Salmaso, I. Toniolo, N. de Cesare, A. Rubini, G.M. De Benedictis, E.L. Carniel, Computational models for the mechanical investigation of stomach tissues and structure, Ann. Biomed. Eng. (2019) 47, doi:10.1007/s10439-019-02229-w.
[30] J.R. Borges, S. Diógenes, E.C.A.O. Bezerra, P.C. Coutinho, T.A. Andrade, C.G.F.D.N. Almeida, M.Â. De Souza, Lower esophageal sphincter pressure measurement under standardized inspiratory maneuveurs, Arq. Bras. Cir. Dig. 28 (2015) 174–177.
[31] J.E. Richter, Techniques in gastrointestinal endoscopy achalasia and lower esophageal sphincter anatomy and physiology : implications for peroral esophageal myotomy technique, Tech. Gastrointest. Endosc. 15 (2013) 122–126, doi:10.1016/j.tgie.2013.04.004.
[32] J.M. Prades, A. Asanau, Anatomia e fisiologia dell'esofago, EMC Otorinolaringoiatr. 10 (2011) 1–14, doi:10.1016/s1639-870x(11)70702-4.
[33] R.E.K. Marshall, A. Anggiansah, C.L. Anggiansah, W.A. Owen, W.J. Owen, Esophageal body length, lower esophageal sphincter length, position and pressure in health and disease, Dis. Esophagus 12 (1999) 297–302, doi:10.1046/j.1442-2050.1999.00060.x.
[34] M. Parikh, R. Issa, A. McCrillis, J.K. Saunders, A. Ude-Welcome, M. Gagner, Surgical strategies that may decrease leak after laparoscopic sleeve gastrectomy: a systematic review and meta-analysis of 9991 cases, Ann. Surg. 257 (2013) 231–237, doi:10.1097/SLA.0b013e31826cc714.
[35] E.L. Carniel, A. Albanese, C.G. Fontanella, P. Giovanni, L. Prevedello, C. Salmaso, S. Todros, I. Toniolo, M. Foletto, Biomechanics of stomach tissues and structure in patients with obesity, J. Mech. Behav. Biomed. Mater. (2020) 103883, doi:10.1016/j.jmbbm.2020.103883.
[36] N. Zijlstra, M. Mars, R.A. De Wijk, M.S. Westerterp-Plantenga, C. De Graaf, The effect of viscosity on ad libitum food intake, Int. J. Obes. 32 (2008) 676–683, doi:10.1038/sj.ijo.0803776.
[37] J. Keller, What is the impact of high-resolution manometry in the functional diagnostic workup of gastroesophageal reflux disease ? Visc Med 34 (2018) 101–108, doi:10.1159/000486883.
[38] B.C. Surjanhata, B. Kuo, Gastrointestinal motility and enteric neuroscience in health and disease, Third Edit (2014), doi:10.1016/B978-0-12-801238-3.00051-9.
[39] J. Desipio, F.K. Friedenberg, A. Korimilli, J.E. Richter, H.P. Parkman, R.S. Fisher, High-resolution solid-state manometry of the antropyloroduodenal region, Neurogastroenterol. Motil. 19 (2007) 188–195 188–195–.
[40] A.W. Goodman, G. Goodman, Generalizations of the theorems of pappus, The American Mathematical Monthly 76 (1969) 355–366 https://doi.org/10.1080/00029890.1969.12000217.
[41] S.H. Emile, W. Ghareeb, H. Elfeki, M. El Sorogy, A. Fouad, M. Elrefai, Development and validation of an artificial intelligence-based model to predict gastroesophageal reflux disease after sleeve gastrectomy, Obes. Surg. (2022), doi:10.1007/s11695-022-06112-x.
[42] A. Shimizu, H. Muramatsu, T. Kura, T. Sakata, Incidence of gastroesophageal reflux associated with percutaneous endoscopic gastrostomy contrast agent viscosity: a randomized controlled crossover trial, Eur. J. Clin. Nutr. 70 (2016) 1057–1061, doi:10.1038/ejcn.2016.76.
[43] J.M. Conchillo, A.J. Smout, Review article: intra-oesophageal impedance monitoring for the assessment of bolus transit and gastro-oesophageal reflux, Aliment. Pharmacol. Ther. 29 (2009) 3–14, doi:10.1111/j.1365-2036.2008.03863.x.
[44] R.K. Goyal, Y. Guo, H. Mashimo, Advances in the physiology of gastric emptying, Neurogastroenterol. Motil. 31 (2019) 1–14, doi:10.1111/nmo.13546.
[45] A. Pretto, I. Toniolo, A. Berardo, G. Savio, S. Perretta, E.L. Carniel, F. Uccheddu, Automatic segmentation of stomach of patients affected by obesity, in: 2023: pp. 276–285. 10.1007/978-3-031-15928-2_24.